Heat Transfer on Small Ribs Mounted On an Adiabatic Plane Channel

Shinya AIBA and Toshihiko SATO *

(平成元年10月31日受理)

1. Introduction

The recent inclination of high heat flux on electronic equipment has requested the precise technique for cooling of it, especially of the IC chips which are in general enveloped by packages. Therefore, it is very important to know the heat transfer around the small blocks situated on the plane wall. There are some works for cooling of the IC packages [1–5]. Most of them studied experimentally with the sublimination method of the naphthalene under the turbulent flow conditions, however. It is well known that the result of heat transfer by the sublimination method is equivalent to that obtained under the constant temperature condition. However, the model should be treated as the constant heat flux in view of the practical cooling of the IC packages. Moreover, the experimental block is too large to simulate the current high heat flux IC package. However, it is very difficult to make the block more smaller, and the measurements of the heat transfer around the block are not accurately conducted.

Yanagida et al. [4] have carried out to estimate the heat transfer of rectangular packages developed along one wall of the flat rectangular duct in low Reynolds number (say, Re=100–300), by the sublimination of naphthalene technique. They also demonstrated the predicted formula of heat transfer. However, their formula is constracted from the assumptions that the heat transfer around the plane wall of the packages is identical with that in the uniform flow field, although the packages are situated on the plane wall.

On the other hand, there have been some studies for the improvement of heat transfer of the duct by roughened surface with small square ribs [6], [8]. However, in most cases the average heat transfer of the duct has been treated only. Therefore, details of heat transfer from the ribs themselves have not been clarified. Furthermore, the flows in the duct have been treated as tubulent ones and the Reynolds numbers handled have not always been small in the previous studies [6], [8].

Most previous works of the cooling for IC packages have been conducted, considering them as three-dimensional. However, the package height has been made small more and more, and the package shapes are not always square as treated in previous works [1–3], [5], but the rectangular types are regular more. In the case of rectangular shapes, it may be possible that the modeling of package is done as two-dimensional when the streamwise pitch between blocks is small.

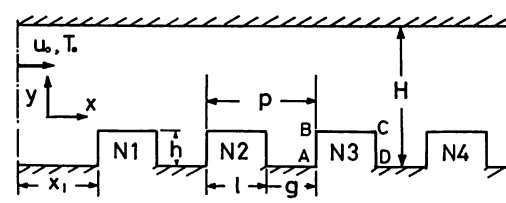

Fig. 1 Schematic diagram and coordinate system with symbol

As a first step, in this paper, numerical

* Former student

analyses were conducted concerning to heat transfer of the small square ribs mounted along one wall of the flat parallel and the adiabatic walls as shown in figure 1 for the purpose of obtaining the fundamental informations for cooling technique of the recent IC package, under the following conditions: the constant heat flux, the low Reynolds number (Re=35–210) and the laminar flow.

Nomenclature

H height of flow passage, Fig.1
h rib height, Fig.1
g gap between ribs, Fig.1
N rib number
Nu $\alpha h/\lambda$ =Nusselt number
Nu' $\alpha' h/\lambda$ =Nusselt number
l rib wide, Fig.1
p rib pitch
Pr Prandtl number
q heat flux
Re Reynolds number=$u_o h/\nu$
T temperature
u velocity component in x-direction
v velocity component in y-direction
x downstream distance
y distance from the wall
X dimensionless distance of stream wide=x/h
Y dimensionless distance from the wall=y/h
α heat transfer coefficient
α' heat transfer coefficient defined by the condition that the objective rib of all the ribs is only heated
ε residue defined in equation (5)
Θ dimensionless temperature= $(T-T_o)/qh$
λ thermal conductivity
ν kinematic viscosity
Ψ stream function
Ω vorticity

subscripts

NW distance between the node of the wall and the node next to the wall
o entrance
w wall

2. Modelled System and Governing Equation

The modelled system employed is shown schematically with the coordinate system in Fig.1. The steady heat transfer in this system with four ribs is treated two-dimensionally, considering the most popular IC package (DIL–P type with 16 pins) [4]. The rib height is kept constant at

3.5㎜ and the rib wide ratio l/h at 1.71. Reynolds number based on h and u_o, which is the entrance flow velocity of air, ranged from 35 to 210, considering the experimental results that the instability of the recirculating flow occurs at the Reynolds number about Re=250–300 obtained by Kang and Chang [9]. The nondimensional pitch p/l was varied from 1.33 to 6.67 (that is, g/l=0.33–5.67). Furthermore, the ratio of duct height H to the rib height h was 5.71. The heat transfer from rib was investigated under the constant heat flux condition.

In the previous data of heat transfer around the block-like electric components which are arranged in in-line [4, 5], we can find that the average Nusselt number of the blocks is in highest at the first row and decrease with increasing downstream distance and is seen to be constant for the second or the third row [4, 5]. Therefore the modelled system in this study is constructed by four ribs as shown in figure 1.

2・1 Differential Equations

In the case of two-dimensional laminar, incompressible and steady state flow, the governing equations of the momentum, and the energy are described following equations with the vorticity equation in Cartesian:

momentum equation,

$$\left(\frac{\partial \Omega}{\partial X}\cdot\frac{\partial \Psi}{\partial Y}-\frac{\partial \Omega}{\partial Y}\cdot\frac{\partial \Psi}{\partial X}=\frac{1}{Re}\cdot\nabla^2\Omega\right) \quad (1)$$

energy equation,

$$\frac{\partial \Theta}{\partial X}\cdot\frac{\partial \Psi}{\partial Y}-\frac{\partial \Theta}{\partial Y}\cdot\frac{\partial \Psi}{\partial Y}=\frac{1}{Re\cdot P_r}\cdot\nabla^2\Theta \quad (2)$$

vorticity equation,

$$\nabla^2\Psi=-\Omega \quad (3)$$

2・2 Boundary Conditions and Numerical Procedures

The approaching length to the first rib x_1 shown in Fig.1 is kept constant at 14.3h for all analyses in the case of four ribs. The boundary conditions of the entrance of duct are $\Psi=Y$, $\Omega=0$, $\Theta=0$ (that is, $T_o=0$). The outlet boundary conditions of the channel are defined as following: gradients of Ψ, Ω and Θ along the stream direction are negligible (i.e. $\partial/\partial X=0$). On the solid boundary, the no-slip condition is applied for the flow field of the system. The condition of the vorticity of the wall is given as [10],

$$\Omega_W=-3(\Psi_{NW}-\Psi_W)/n_{NW}^2-0.5\,\Omega_{NW} \quad (4)$$

The temperature condition of rib was assumed as constant heat flux, that is, $\Theta_W=\Theta_{NW}+n_{NW}$, when the rib was heated. Other thermal boundary condition of the walls except the surface of the ribs may be written $\partial\Theta/\partial Y=0$. Where, subscript NW denotes the neighbouring

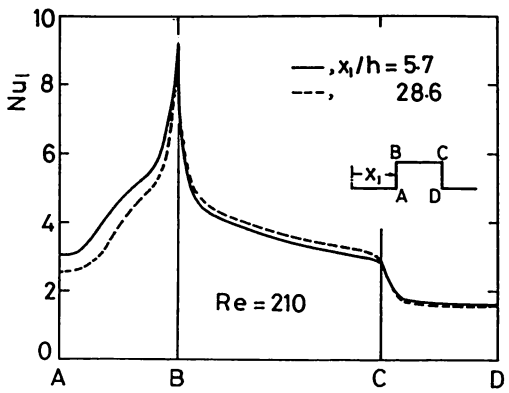

Fig. 2 Local Nusselt Number distributions of single rib with x_1/h for Re=210

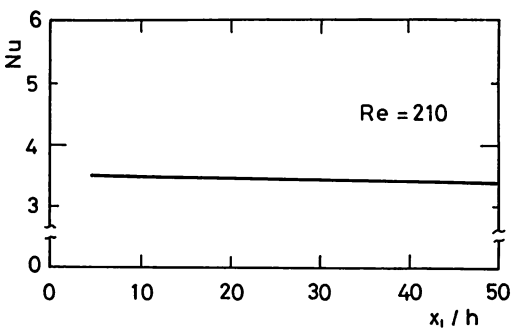

Fig. 3 Average Nusselt Number of all over the surface of single rib with x_1/h for Re=210

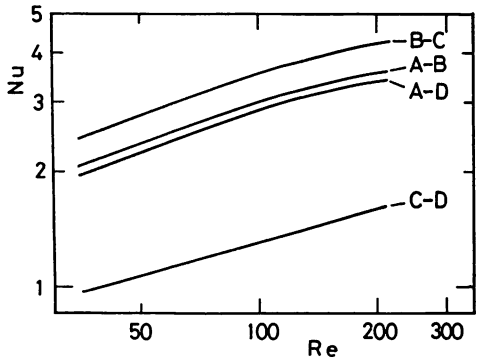

Fig. 4 Average Nusselt number results of A—B, B—C, C—D and A—D with Re

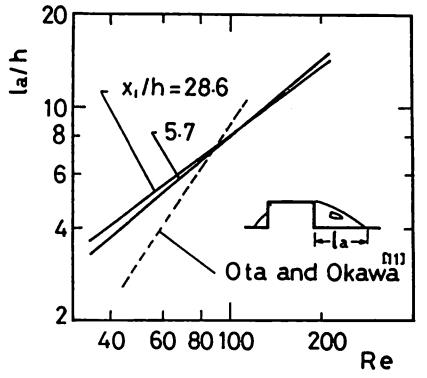

Fig. 5 Variation of reattachment length from rib with Re

node and n_{NW} represents the normal distance between the node of the wall and the node next to the wall.

The governing equations with the boundary conditions are solved using the finite difference scheme described in reference [10]. In the scheme, the upwind method is applied to the convective term and the central difference is used to the diffusion one. Non-uniform grid nodes (74×18) are chosen, and the grids near the wall and the corner are fine. The grid size ranges from ΔX/H (or ΔY/H)=0.025 to 0.1. The Gauss-Siedel iteration method has been applied for obtaing a convergence of Ψ, Ω and Θ. The convergence criterion of these variables is defined as

$$\varepsilon = |(\Phi^n - \Phi^{n-1})/\Phi^n|_{max} \qquad (5)$$

where, n is the nth iteration. The residual ε is 10^{-4} for Ψ, Ω and is 10^{-5} for Θ. An averaging method has been used in oder to obtain the variables of the corners of rib.

3. Results and Discussion

The computational results of the velocity distribution for laminar flow in the inlet section of the straight channel were obtained in order to compare with the exact solution of it. It was confirmed that there were good agreements with each other. Before describing the results obtained from four ribs, it may be necessary to show the behaviors of heat transfer in the case of a single rib, as a first step. Figure 2 shows the variations of local Nusselt number Nu_l around the rib for the Reynolds number Re=210. In the figure, the symbols A, B, C and D indicate the corner of rib, respectively, and x_l/h denotes the dimensionless distance from the inlet of the duct to the front face A–B of the rib. It can be seen that Nu_l of the corner B is very large and independent on x_l/h. This is resulted from the abrupt variations of the velocity around that corner. Nu_l of the A–B wall in the case of x_l/h=5.7 is larger about 10–20 percent than that for x_l/h=28.6. It is considered that the velocity of oncoming flow to the A–B wall for x_l/h=5.7 is larger than that for x_l/h=28.6. That is, the boundary layer thickness (which is the thickness when the rib does not exist on the wall of channel) at the point of x_l/h=5.7 is almost identical to the height of rib, while the thickness for x_l/h=28.6 is about 1.7h. However, the undisturbed maximum velocity in the parallel channel increases with increasing of the distance from the entrance, in the inlet region of the channel. Therefore, Nu_l of the B–C wall for x_l/h=28.6 shown by the dotted line is almost larger than that for x_l/h=5.7, because the undisturbed maximum flow velocity

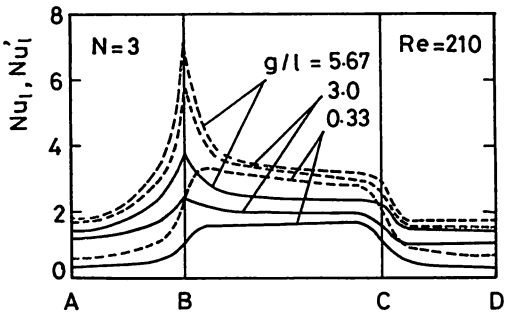

Fig. 6 Local Nocal number destributions of the third rib with g/1 for Re=210

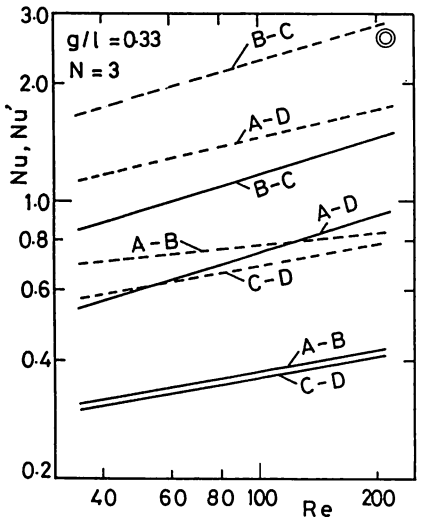

Fig. 7 Average Nusselt number results of A—B, B—C, C—D and A—D with Re for N=3, g/1=0.33; ◎, Yanagida et al.[4]

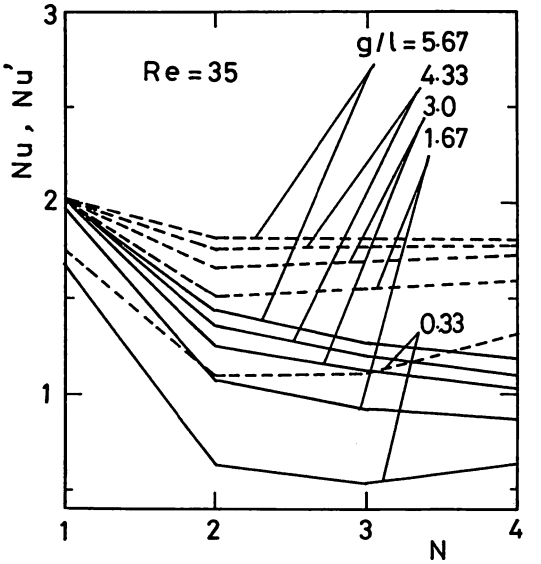

Fig. 8 Variation of average Nusselt number of all over the surface of each rib with N for Re=35

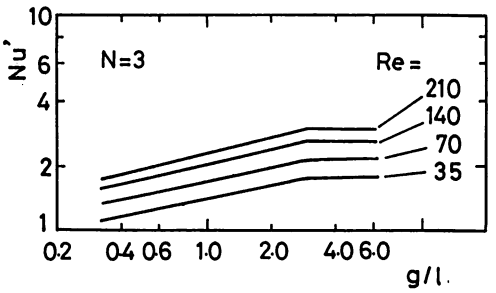

Fig. 9 Variation of Nu' with g/1 and Re for N3

mentioned above is accelerated about 10 percent than that of the entrance of the channel. It is found that Nu_1 of the C—D surface is almost independent of x_1/h. It has been also confirmed that the distributions of Nu_1 do not vary with x_1/h in the range x_1/h=28.6—48.6.

Average Nusselt number Nu around the entire surface of the rib (that is, A—B—C—D) is described in Fig.3, for Re=210 with x_1/h. It can be seen that the result of Nu changes little by x_1/h, although it decrease somewhat with increasing of x_1/h. Figure 4 indicates the dependency of Nusselt number for Reynolds number. In the figure, the symbol A—D (shortening of A—B—C—D) indicates the entire surface of rib. Nu of the B—C wall show the highest value and Nu of the C—D wall is considerably smaller than that of other walls. It can be seen that the relations between Nu and Re are not always linear except the result of C—D wall.

It is important to know the reattachment length of the shear layer from the rib to the duct wall in relation to the design of rib arrangement in practice [4]. Figure 5 demonstrates the length of reattachment point la/h with Reynolds number. In the range of Re=35—210, la/h is linearly increasing with Re. However, the inclination of la/h for Re in case of x_1/h=5.7 is somewhat

larger than that of $x_1/h=28.6$. The dotted line is the result shown by Ota et al.[11], which is the reattachment length of shear layer from the leading edge of the blunt flat plate in the uniform flow field. Their definition of the Reynolds number is based on the half thickness of the plate. The dependency of $\ell a/h$ for Re of that case is stronger than the results treated herein.

Figure 6 describes the typical local Nusselt number distributions around the third rib (N=3 or N3) of four ribs with Re=210 for the dimensionless gap g/1. The results shown by the dotted line indicate that the third rib is only heated, and the results by the solid line do that all the ribs are uniformly heated. That is, Nu_1' means the result obtained under the condition that the objective rib is only heated.

In previous studies concerning to the cooling of the block-like electronic packages [4,5], the heat transfer rates around these are seen to be constant for the second or the third row when the objective package is only heated. Therefore, in this report the results of the third rib are mainly discussed, considering also the effects of downstream rib behind N3. In the figure, it is seen that the distribution of Nu_1' for g/1=5.67 is similar to that of the single rib as shown in Fig.2. The maximum of Nu_1' at the corner B does not appear when g/1 is very small such as 0.33 and the value of Nu_1' for g/1=0.33 is considerably lower than that of other gaps, especially in the upstream surface of the rib. On the other hand, the results of Nu_1 shown by the solid lines are small in general due to the heating of other ribs (especially of the first and the second ribs), comparing with these of Nu_1'.

Average Nusselt numbers for g/1=0.33 are shown in Fig.7 with Reynolds number. The symbols and the lines in the figure are identical with these of Figs.4 and 6. It is found that these average Nusselt numbers of A–B, B–C, C–D and A–D increase linearly with increasing of Reynolds number and the tendency of them is different from the case of single rib shown in Fig.4. The dependency of these Nu, Nu' for Re is strong in the upper surface of the rib (B–C), where the heat transfer rate is considerably larger than these of A–B and C–D surfaces. Therefore, the behaviors of Nu' and Nu around the entire rib are influenced by these of B–C surfaces.

In the figure, the symbol of ◎ shows the result obtained from the three-dimensional block by Yanagida et al.[4]. Thier result have been obtained as following. The dimensions of the block are for H=20㎜, h=3.5㎜, l=6.3㎜, g=3.7㎜ and the length perpendicular to l is about 5.5h. The heating condition is equivalent to constant temperature since the naphthalene sublimination method has been used. Furthermore, their block arrangement is in-line. The result shown in the figure corresponds to Nu' of A–D. Their experimental result is higher about 60 percent than that of the present study. This difference may be explained by the facts that the heat transfer of the side walls of block (perpendicular to the stream direction) is not negligible and that increase of heat transfer is caused by the three-dimensional flow around the block, especially downstream surface of the rib. However, it may be considered that the influence by the flow difference decreases when the gap between ribs is small.

Figure 8 shows the variations of average Nusselt number of A–D for each rib with g/l when the Reynolds number is equal to 35. Nu and Nu' of N1 (which indicates the first rib) are almost identical with Nu of the single rib as shown in Fig.4 for $g/l \geqq 1.67$. It can be seen that the results for the second rib N2 decrease affected by N1. That is, N2 is buried in the separated flow region (in which, the flow is very stagnant) of N1. These trends have been confirmed in the high Reynolds number ($Re \sim 10^4$) when the bluff bodies are mounted on the plane wall, although the system treated is somewhat differenct from the present study [12]. Furthermore, the thermal wake from N1 cause to decrease the value of Nu of N2, when all the ribs are heated and g/l is small. Nu value of N2 for g/l=0.33 is about 0.38 times of that of N1 for example. Nu decreases in

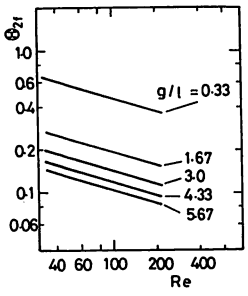

Fig. 10 Results of Θ_{2f} with Re

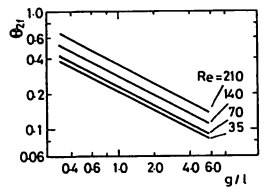

Fig. 11 Results of Θ_{2f} with g/1

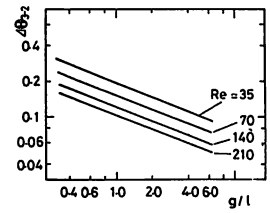

Fig. 12 Results of $\triangle\Theta_{3-2}$ with g/1

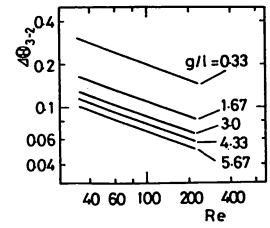

Fig. 13 Results of $\triangle\Theta_{3-2}$ with Re

general with increasing of N (except the Nu for N4). It has been found that thus tendencies are independent of Reynolds number.

Nu' for N3, N4 (the fourth rib) change little by N (except the case Nu' of N4 for g/l=0.33). These trends can be seen in the previous studies [4,5]. The results of N4 are somewhat larger than these of N3 when g/l is small, although N4 is located downstream of N3. It may be considered that the heat transfer of the rear face of N4 increases because the flow downstream of N4 is not stagnant caused by no presencee of the ribs behind N4. Moreover, it is obvious that the heat transfer increases with increasing of g/l, but the increasing ratio decreases with increasing of g/l and saturates for g/l$>$3.0. When Re takes large value, the values of Nu' change little for g/l$\geqq$3.0 as shown in Fig.9 (in which Nu' with N3 are indicated against g/l). In the range g/l=0.33$\sim$3.0, however Nu' increase linearly with increasing of g/l independent of Re and there exists such a relation Nu' $\propto (g/l)^{0.237}$. Furthermore, it can be found that Nu' $\propto Re^{0.312}$ in the ranges of g/l=0.33$\sim$5.67 and Re=35$\sim$210. Therefore, Nu' of N3 are written as

$$Nu' = 0.448\,(g/l)^{0.237}.\ R_e{}^{0.312} \tag{6}$$

for the range g/l=0.33$\sim$3.0,

$$Nu' = 0.581 R_e{}^{0.312} \tag{7}$$

for the range 3.0$<$g/l$<$6.0.

These results shown in equations (6), (7) may be considered as those for the ribs downstream of N3 as suggested in Fig. 8.

Attention will now be focused on the relation between the results of Nu' and those of Nu. It is more convenient to use Nu than Nu' owing to design the thermal equipments in practice. The dimensionless temperature of oncoming flow towards the rib is designated as θ_{Nf} hereafter, when all the ribs are heated. θ_{1f} which denotes the temperature for N1 is equal to θ_0. θ_{Nf} for the Nth rib increases of course with increasing N. If the differences between θ_{3f} and θ_{2f} are defined by $\triangle\theta_{3\text{-}2}$, θ_{3f} is described as

$$\theta_{3f} = \theta_{2f} + \triangle\theta_{3\text{-}2} \tag{8}$$

Furthermore, if the similar definition for $\triangle\theta_{4\text{-}3}$ is made, θ_{4f} is given as

$$\theta_{4f} = \theta_{3f} + \triangle\theta_{4\text{-}3} \tag{9}$$

When the heat flux from each ribs is equal, the temperature difference $\triangle\theta(=\theta_{Nf}-\theta_{N\text{-}1,f})$ may be considered equal. Then, it can be written that $\triangle\theta_{3\text{-}2} = \triangle\theta_{4\text{-}3} = \triangle\theta$. Therefore, θ_{3f}, θ_{4f} are described as

$$\theta_{3f} = \theta_{2f} + \triangle\theta \tag{10}$$

$$\theta_{4f} = \theta_{2f} + 2\triangle\theta$$

that is, $\theta_{Nf} = \theta_{2f} + (N-2)\triangle\theta$ (11)

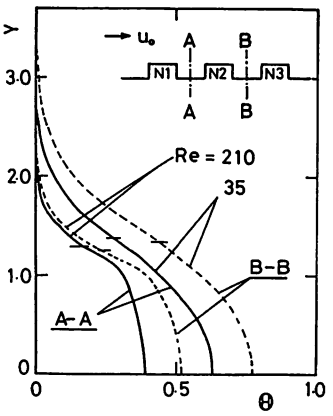

Fig. 14 (a) Dimensionless temperature distributions with g/l=1.67 for Re=35, 210

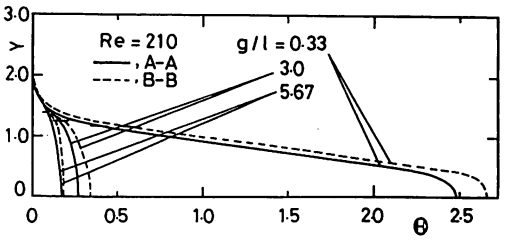

Fig. 14 (b) Dimensionless temperature distributions for Re=210 with g/l=0.33, 3.0, 5.67

where, $N \geqq 2$.

On the other hand, the average Nusselt number obtained by using θ_{Nf} under the condition that all the ribs are heated may be equal to Nu_N' calculated from the condition that only the objective rib is heated [13]. Therefore, there exists following relation between Nu_N and Nu_N'

$$Nu_N = 1/(1/Nu_N' + \theta_{Nf}) \tag{12}$$

where, subscript N denotes the Nth of rib.

From this, if θ_{Nf} is obtained, Nu will be calculated from equation (6) or (7) for example.

In this study, it is most reasonable that $\triangle\theta$ shown in equation (11) is replaced by the temperature difference $\triangle\theta_{3\text{-}2}(=\theta_{3f}-\theta_{2f})$. On the other hand, θ_{2f} is given as

$$\theta_{2f} = 1/Nu_2 - 1/Nu_2' \tag{13}$$

From the results of Nu_2 and Nu_2', θ_{2f} are obtained and demonstrated in Figs. 10 and 11 as the functions of g/l and Re. As a result, θ_{2f} is given as

$$\theta_{2f} = 1.01\,Re^{-0.296}\,(g/l)^{-0.53} \tag{14}$$

within $\pm$5 percent error band.

θ_{3f} is also obtained by the similar manner as θ_{2f}. $\triangle\theta_{3\text{-}2}(=\theta_{3f}-\theta_{2f})$ are described in Figs. 12, 13, and presented as

$$\triangle\theta_{3\text{-}2} = 0.737\,Re^{-0.366}\,(g/l)^{-0.40} \tag{15}$$

with an extreme deviation of 5 percent. Therefore, θ_{Nf} yields

$$\theta_{Nf} = 1.01Re^{-0.296}(g/l)^{-0.53} + 0.737\,(N-2)\,Re^{-0.366}\,(g/l)^{-0.40} \tag{16}$$

where, $2 \leqq N < 4$.

Nu_N can be obtained from equations (12) and (16) with Nu_N' shown by equations (6) and (7).

In order to know the behaviors of θ_{Nf}, typical distributions of the dimensionless temperature in the center sections between the ribs are shown for g/l=1.67 in figure 14(a). The solid lines present the temperature distributions at the section A–A (center section between N1 and N2) and the dotted lines at the section B–B (center section between N2 and N3). The distributions for Re=35 show that the temperature field diffuses towards the main flow at about Y=2.5~3.5, while the case of Re=210 at about Y=2.0. Moreover, when Re is large the temperature decreases abruptly at about $Y > 1.0$. In the figure, the positions of θ_{Nf} are shown by the horizontal bar symbol (–). They are located in the neighborhoods of Y=1.3 which is larger than the levels of the dividing stream line, which is situated at about Y=1.0 for g/l=1.67 independent of Reynolds number treated herein.

The effect of g/l for temperature distributions is presented in Fig.14(b) for Re=210. It is obvious that θ for g/l=0.33 is very large in the range $Y < 1.2$, and θ decreases with increasing g/l.

The locations of θ_{Nf} are from Y=1.1 to 1.4, and they approach to the direction of Y=0, when g/l and Re are small. Furthermore, it can be recognized that θ_{Nf} at the section B–B generally are located at the smaller Y than the case at the A–A section.

4. Concluding Remarks

Heat transfer of the small square ribs mounted on one side of the parallel flat walls which are adiabatic has been calculated numerically in the laminar flow field. The local and average Nusselt numbers around ribs have been obtained varing the gap between ribs and Reynolds' number under the constant heat flux. The results of average Nusselt number Nu' which are obtained by heating only the objective rib show that the behaviors of the first rib are identical with these of the single rib except the case when the gaps are very small, and that the average Nusselt numbers Nu' of the ribs behind the first rib are constant values. Nu' of the third rib are evaluated by the equation (6) or (7). When all the ribs are heated, the average Nusselt numbers Nu of the first rib are similar to the behaviors of Nu'. Nu of the ribs behind the first rib decrease especially when the gaps between ribs are small. The relations between Nu and Nu' for the Nth rib are obtained by the equation (12), by considering the characteristic temperature as described in equation (16).

References

1. Sparrow, E. M., Niethammer, J. E. and Chaboki, A., Int. J. Heat Mass Transf., 25(1982) 961–973.
2. Arvizu, D. E. and Moffat, R. J., Electron Components Conf., 32(1982)133–144.
3. Sparrow, E. M., Yanezmoreno, A. A. and Otis, JR. D. R., Int. J. Heat Mass Transf., 27(1984) 469–473.
4. Yanagida, T., Nakayama, W. and Nemoto, T., Trans. JSME, 54(1984)1294–1301.
5. Torikoshi, K., Kurihara, T. and Nemoto, T., 24th National Heat Transfer Symposium of Japan, (1987)100–102.
6. Donne, M. Dalle and Meyer, L., Int. J. Heat Mass Transf., (1977)587–620.
7. Han, J. C., Glicksman, L. R. and Rowsenow, W. M., Int. J. Heat Mass Transf., 21(1978) 1143–1156.
8. Berger, F. P. and Hau, K.– F., F.– L., Int. J. Heat Mass Transf., 22(1979)1645–1656.
9. Kang, In Seok and Chang Ho Nam, Int. J. Heat Mass Transf., 25(1982)1167–1181.
10. Gosman, A. D., Pun, W. M., Runchal, A. K., Spalding, D. B. and Wolfshtein, M., Heat and Mass Transfer in Recirculating Flows, Academic Press. New York 1969.
11. Ota, T. and Okawa, Y., Bull. of the JSME 24(1981)941–947.
12. Aiba, S., JSME International Journal 30(1987)1943–1950.
13. Aiba, S. and Yamazaki, Y., Trans. ASME. J. Heat Transf. 98(1976)503–508.